



HAL
open science

EIC + , an algorithm for automatic and unsupervised extraction of ion chromatograms in high resolution mass spectrometry

Jean-Claude Boulet

► **To cite this version:**

Jean-Claude Boulet. EIC + , an algorithm for automatic and unsupervised extraction of ion chromatograms in high resolution mass spectrometry. *International Journal of Mass Spectrometry*, 2021, 469, 10.1016/j.ijms.2021.116672 . hal-03428111

HAL Id: hal-03428111

<https://hal.inrae.fr/hal-03428111>

Submitted on 2 Aug 2023

HAL is a multi-disciplinary open access archive for the deposit and dissemination of scientific research documents, whether they are published or not. The documents may come from teaching and research institutions in France or abroad, or from public or private research centers.

L'archive ouverte pluridisciplinaire **HAL**, est destinée au dépôt et à la diffusion de documents scientifiques de niveau recherche, publiés ou non, émanant des établissements d'enseignement et de recherche français ou étrangers, des laboratoires publics ou privés.



Distributed under a Creative Commons Attribution - NonCommercial| 4.0 International License

EIC+, an algorithm for automatic and unsupervised extraction of ion chromatograms in high resolution mass spectrometry

Jean-Claude Boulet¹

SPO, INRAE, Univ Montpellier, Institut Agro, Montpellier, France

INRAE, PROBE Research Infrastructure, Polyphenol Analytical Facility, Montpellier, France

Abstract

Within the feature extraction process in high-resolution mass spectrometry (HRMS), we focused on the identification of EICs-Extracted Ion Chromatograms. A proposed algorithm tuned with its default parameters yielded EIC matrices which recovered most of the 836 reference features identified within a set of public and fully described Orbitrap data, already benchmarked with XCMS, MZmine2, MS-Dial and Compound Discoverer. A good accuracy on the calculation of the m/z values was also observed. Tools are available on the Galaxy Test Toolshed.

Keywords: extracted ion chromatograms; features; m/z values; high resolution mass spectrometry; EIC+ algorithm

1. Introduction

2 A mass spectrum is a beam of abundances of ions represented by their m/z
3 values [3]. Within each mass spectrum, the regions of m/z values with high
4 abundances, or signals, form mass peaks, or peaks. HRMS-high resolution mass
5 spectrometry consists in liquid chromatography coupled to mass spectrometry.
6 The analysis of a sample in HRMS yields a MS data, which is a series of mass
7 spectra, each acquired at a different retention time (RT). A collection of several
8 MS data will form a MS dataset. Within each MS data, a feature is defined
9 when a same peak is identified in several mass spectra which are consecutive
10 by their RTs. A feature is a triplet containing a m/z value, a retention time
11 and a signal intensity. Extraction of features, performed by proprietary or free
12 softwares, is the beginning of HRMS preprocessings. It can be summarized as
13 follow for a MS1 acquisition (full scan). Let ms_i be the mass spectrum corre-
14 sponding to the i^{th} retention time. Each ms_i is a matrix of two columns, m/z

Email address: jean-claude.boulet@inrae.fr (Jean-Claude Boulet)

Preprint submitted to Elsevier

June 24, 2021

15 values and signal intensities, which form peaks with the profile option of the
16 mass spectrometer, or which have been converted to centroids with the centroid
17 option. Successive ms_i , e.g. ms_i , ms_{i+1} and ms_{i+2} , may contain the same
18 m/z value. From a MS1 data and a given m/z value, an Extracted Ion Chro-
19 matogram or EIC is obtained by collecting the signals associated to a given m/z
20 value (with a tolerance) along all the RTs. The next process is the identification
21 of features or chromatographic peaks, sometimes referred to as peak picking. But
22 the calculation is tricky, and several softwares, or even the same software with
23 different parameters, do not yield the same solution. Benchmarks give clues on
24 their respective performances, according to different figures of merit. A first ap-
25 proach was to compare the features obtained by different softwares, using their
26 distances calculated with their m/z and RT values. The figure of merit was the
27 number of features identified by several softwares, considered to be true posi-
28 tives. Venn diagrams were used by Tautenhahn et al [8] to compare Centwave,
29 MZMine and Matchfilter algorithms, and by Myers et al [4] to compare XCMS
30 [7] and MZmine2 [6]. But an outlier on Venn diagrams is simply an algorithm
31 which performs differently; its performances can be worse, or better. Then, an-
32 other and more reliable approach was based on a ground truth, reference values
33 to which experimental results could be compared. Li et al [2] compared sev-
34 eral softwares on samples for which hundreds of compounds had been manually
35 quantified. The figure of merit was the recovery rate of features, based on the
36 proximity between reference and experimental values for three variables: RTs,
37 m/z and signal intensities. Such approach targets final users, because it gives
38 them clues to choose a processing application. But it does not explain why an
39 application performed better than another. In other words, we have seen that
40 features extraction is a two-steps process: EIC extraction from raw MS data
41 then features identification from EICs. The recovery rate was not 100% for any
42 software: where was information lost? At the EIC step? At the features step?
43 Both? Moreover, the accuracy of m/z prediction was not discussed, while it
44 should be a mandatory figure of merit when the goal of the processing is to
45 propose CHONS chemical formula.

46 Taking those remarks in consideration, the design of the following algorithm
47 was focused on the EIC extraction and the accuracy of the prediction of the
48 m/z values, with a parsimonious number of tuning parameters. The aim of this
49 article was to show that almost all information from the dataset published by
50 Li et al could be recovered by the EICs, and beyond, that it remains possible
51 to improve the features extraction process.

52 2. Material and methods

53 2.1. The EIC+ algorithm

54 Contrary to ADAP [5] or Centwave [8] which process each data once, our
55 algorithm performs several processings of the original centroid data. The goal
56 was to determine more accurately the experimental m/z values leading to the
57 future EICs. At each loop, m/z values were recalculated, converging towards

58 stable values. The algorithm called *EIC+* is schematized in figure 1. The three
59 tuning parameters were: *mztol*, *eicsig* and *dw*, i.e. a tolerance around a given
60 *m/z* value, a minimum of signal and a Durbin-Watson threshold. The starting
61 point was a centroid high resolution MS data.

- 62 • Identification of a first *m/z* list
63 All the signals of the MS data were gathered into the same matrix of two
64 columns: *m/z* values and signal intensities. The *m/z* values were sorted
65 in ascending order, identical *m/z* values were merged, signal intensities
66 added. The maximum of signal was associated to a *m/z* value called
67 mz_{max} which was stored in a list of *m/z*. The *m/z* between the bound-
68 aries [$mz_{max}-mztol$, $mz_{max}+mztol$] were dropped. Then, the algorithm
69 checked for the next mz_{max} and the previous calculations were repeated
70 until the maximum of the remaining signals reached *eicsig*.
- 71 • Filling a first EIC matrix
72 The first EIC matrix was initiated as a matrix of zeros; the rows were the
73 retention times, and the columns the list of mz_{max} previously identified.
74 The MS data was scanned again, each *m/z* value was compared to the
75 *m/z* of the EIC matrix. If an absolute difference was lower than *mztol*, the
76 signal was added into the EIC matrix at the corresponding retention time
77 and *m/z*; otherwise it was discarded. Some statistics were also collected.
- 78 • Converging towards a last EIC matrix
79 The statistics allowed a new barycentric calculation of each *m/z* value of
80 the previous EIC matrix. Two EICs which became closer than *mztol* were
81 merged into a new and temporary EIC whose *m/z* value was recalculated
82 by weighting the *m/z* with the signals used to fill the matrix. After ex-
83 ploring all of the possibilities of merging EICs, a new EIC matrix was
84 initiated to zeros and filled as previously described. Several loops were
85 processed until a stop, no more than 5 *m/z* values merged in 3 successive
86 loops. The last EIC matrix was obtained.
- 87 • Cleaning up the last EIC matrix
88 The cleaning was achieved using a slightly modified version of the Durbin-
89 Watson (DW) test. For each EIC forming a vector of length N_{RT} (the
90 number of retention times), a vector of length $N_{RT} - 1$ containing the
91 differences between two successive elements was calculated. The DW value
92 was the ratio between the norm of the difference vector and the norm
93 of the EIC vector. It ranged from 0 for continuous signals to 2 for very
94 discontinuous signals. EICs with DW values higher than *dw* were supposed
95 to be noise, so they were dropped.

96 2.2. Feature extraction from the EICs

97 Regular outputs from e.g. XCMS or MZMine2 are features, while regular
98 outputs for *EIC+* are matrices of EICs, the step before. Our goal was to show

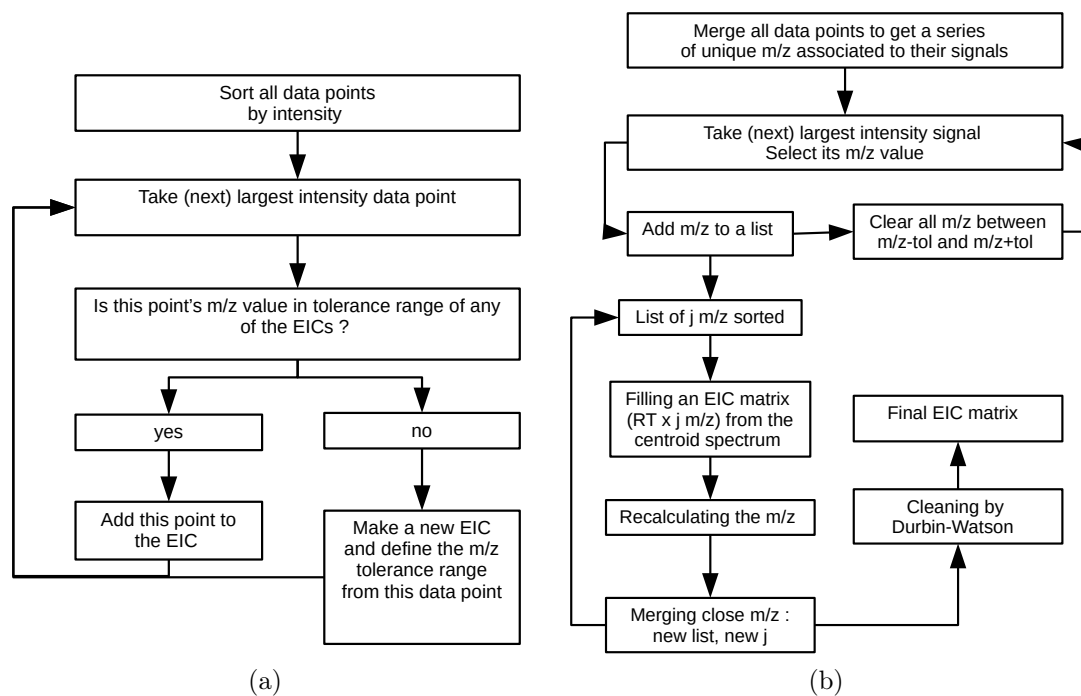


Figure 1: Flow diagram of MZmine2-ADAP (a) and of *EIC+* (b). The ADAP flow diagram was reproduced from figure 1 of Myers et al, *Anal.Chem.*, 2017. The box "Filling an EIC matrix" in (b) performs almost the loop of the ADAP algorithm in (a), with the difference that, in case of "no", ADAP makes a new EIC with the data point whereas *EIC+* drops it.

109 that a large part of the information concerning the reference features had been
100 captured within the EIC matrix. For comparison with the results obtained by
101 Li et al [2], features extraction from our EIC matrices was mandatory. It was
102 performed with a home-made tool, designed to be plugged into the workflow,
103 not described because we do not claim any novelty with it. The results were
104 good enough to use it, even if other algorithms may have performed better. To
105 save calculation time, a selection of the EICs corresponding to the reference
106 m/z values was performed on the EIC matrix before features extraction.

107 2.3. The MS datasets

108 Two MS datasets were considered. MS dataset 1 consisted in a single
109 Orbitrap MS data, named *VI2016_AC_4A.raw* acquired at the University
110 of Barcelona in 2016. The sample was a red wine spiked with acetaldehyde
111 prior to its analysis. Polyphenols had been targeted, 117 compounds had
112 been previously manually identified in this wine sample, following a previous
113 work on model solutions [9]. Nevertheless, as several chemical compounds
114 had exactly the same raw formulae, the number of different m/z values was
115 109. MS dataset 2 consisted in ten Orbitrap MS datasets described by Li et
116 al [2], and available with their metadata thanks to the Metabolights project
117 at: <https://www.ebi.ac.uk/metabolights/MTBLS733>. The spectra were named
118 *SA1.raw* to *SA5.raw* and *SB1.raw* to *SB5.raw*. The metadata consisted in a
119 list of 836 chemical compounds manually identified by Li et al into the 10 spec-
120 tra, with their RTs, m/z values and signal intensities. Only MS1 spectra were
121 considered. Before processing, two successive conversions were performed: from
122 .raw to .md5 by MSConvert, then from .md5 to .h5 by HDFView.

123 2.4. The processings

124 All tools were coded in Scilab 6.0.2 (<https://www.scilab.org>) with the Fact
125 toolbox, then wrapped into Galaxy tools. The centroid calculation was per-
126 formed according to a previous work [1].

127 2.5. Tuning the EIC+ with dataset 1

128 The workflow concerning dataset 1 involved EIC extraction only, features
129 were not considered yet. The development and the very first application of
130 *EIC+* was based on dataset 1 and the figures of merit described hereafter.
131 Preliminary experiments had concluded that the minimum of signal *eicsig* and
132 the Durbin-Watson threshold *dw* could be fairly set to 30000 and 1 respectively.
133 Variations around these values did not strongly modify the results (not shown).
134 Our attention was focused on *mztol*. Values were chosen from 0.0012 to 0.0060
135 by steps of 0.0012. The algorithm was run with each of these values, yielding for
136 each *mztol* a list of experimental m/z values. Then, each reference m/z value
137 was sought within these lists with m/z tolerances set to 0.0005, 0.0100, 0.0030,
138 0.0050 and 0.0100.

139 *2.6. The benchmark, with dataset 2*

140 The processing consisted in two successive steps: 1) extracting the EICs with
141 *EIC+*; 2) extracting the features from the previously determined EICs.

142 *2.6.1. Step 1: extracting the EICs with EIC+*

143 The workflow concerning MS dataset 2 is described in figure 2. Compression
144 was a means to save computational resources and time. It consisted in merging
145 5 successive RTs. When EICs had been extracted from each of the 5 datasets,
146 they were averaged, yielding a single EIC file from SA and a single EIC file from
147 SB. Then, features could be extracted.

148 *2.6.2. Step 2: extracting the features*

149 The features were extracted with a home-made tool using 4 parameters: i)
150 the minimum and maximum sizes of the RT window, $0.3mn$ and $0.05mn$ respec-
151 tively; ii) thresholds for the maximum of signal in each selected feature/peak
152 and for the Durbin-Watson value, 100000 and 1 respectively.

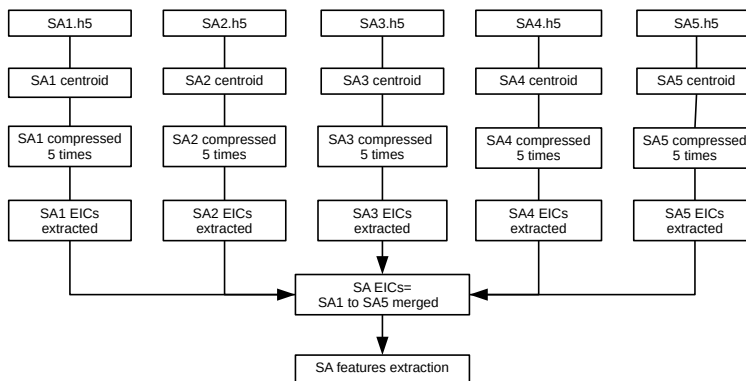


Figure 2: Workflow applied to SA1-SA5. SB1-SB5 were processed similarly.

153 *2.7. The figures of merit*

154 Five figures of merit were calculated. The EICs m/z recovery and the EICs
155 m/z unicity ratio were applied to dataset 1 for tuning the parameters, and to
156 dataset2 for assessing the quality of EICs extraction. The true features, the
157 accurately quantified true features and the RMSEP-root mean square error of
158 prediction of the true features m/z values were applied to dataset 2 after features
159 extraction.

- 160 • The EICs m/z recovery

161 The EIC recovery is N_R the number of chemical compounds identified by
162 the processing. It should be compared to the total number of reference
163 m/z values.

- The EICs m/z unicity ratio

The i^{th} m/z value from the m/z reference list of chemical compounds can be associated to N_u^i m/z values of the EIC matrix, under a certain tolerance. The not-null N_u^i values were added and divided by N_R , yielding the unicity ratio:

$$\text{unicity ratio} = \frac{\sum N_u^i}{N_R}$$

164 A ratio close to 1 suggests that there is non ambiguity of identification
 165 between the m/z values from the reference list and the m/z values from
 166 the EIC matrix.

- True features and accurately quantified true features

167 Our experimental features were compared to the reference features pro-
 168 vided by Li et al on the basis of their m/z values, their retention times
 169 and their signal intensities. According to the same authors, true features
 170 verified simultaneously shifts in m/z values and RTs lower than thresholds
 171 set to 10 ppm and 0.3 minutes respectively. One of our first motivations
 172 was to determine chemical compositions from the molecular weights of the
 173 ions, so we compared the m/z values on the basis of a mass unit, rather
 174 than of a percent which depends on the m/z values. For a comparison as
 175 fair as possible with the previous benchmark of Li et al, the median of the
 176 836 reference m/z values was calculated, the value of 386 obtained. There-
 177 fore, the threshold was set to 10 ppm of 386, that is 0.00386 mass units.
 178 For the retention times, no threshold was used. Our algorithm provided
 179 the start and stop RTs, the test was passed when the reference RTs fell
 180 within this range. Then, accurately quantified true features corresponded
 181 to true features for which the experimental SB/SA signal ratio did not
 182 differ from more than 20% from the reference ratio determined manually
 183 by Li et al and referred to as fold changes in their data.
 184

- The RMSEP of the true features m/z values

185 Let \mathbf{m}_{ref} and \mathbf{m}_{exp} be vectors containing the N reference m/z values and
 186 the N experimental m/z values associated to the N true features defined
 187 above. The RMSEP-root mean square error of prediction was calculated
 188 for SA then for SB according to Equation 1, with $\mathbf{d} = \mathbf{m}_{ref} - \mathbf{m}_{exp}$.
 189

$$RMSEP = \sqrt{\frac{\mathbf{d}^T \mathbf{d}}{N}} \quad (1)$$

190 3. Results and discussion

191 Results concerning the tuning of the parameters for dataset 1 were gathered
 192 into table 1. The best solution should present the highest recovery percent and
 193 the lowest unicity ratio, while $mztol$ being as low as possible: $mztol = 0.0024$
 194 was chosen. Then a processing of dataset 2 was performed with the parameters
 195 defined above, i.e. $mztol = 0.0024$, $eicsig = 30000$ and $dw = 1$, which are also

EICs m/z recovery						EICs m/z unicity ratio					
$mztol$	m/z tolerance, $\times 10^{E4}$ with reference values					$mztol$	m/z tolerance, $\times 10^{E4}$ with reference values				
	5	10	30	50	100		5	10	30	50	100
0.0012	23	50	93	94	95	0.0012	1	1	1.06	1.18	1.23
0.0018	24	55	94	98	99	0.0018	1	1	1.03	1.12	1.17
0.0024	26	55	100	103	103	0.0024	1	1	1.01	1.07	1.16
0.0030	26	59	98	102	103	0.0030	1	1	1	1.05	1.13
0.0036	27	63	101	105	106	0.0036	1	1	1	1.05	1.10
0.0048	31	66	101	105	106	0.0048	1	1	1	1.01	1.08
0.0060	33	62	103	106	108	0.0060	1	1	1	1.00	1.05

Table 1: Two figures of merit calculated for dataset 1. The number of different m/z values from the reference list is 109.

196 the default parameters. This choice was supported by similar results previously
197 obtained on two other datasets, not reported here. Using the *EIC+* algorithm,
198 two EIC matrices \mathbf{X}_{sa} and \mathbf{X}_{sb} of dimensions (2484×19958) and (2475×18773)
199 were obtained from the five SA and the five SB MS data of Li et al, respectively.
200 The first value was the number of retention times, the second the number of
201 EICs. \mathbf{X}_{sa} presented 800 EICs, and \mathbf{X}_{sb} 799, whose m/z values corresponded
202 to reference features, see table 2.

Dataset	\mathbf{X}_{sa}	\mathbf{X}_{sb}
Total number of EICs	19958	18773
Number of selected EICs	800	799
Unicity ratio	1.015	1.011
RMSEP of m/z values	0.00044	0.00044
DW value	0.27	0.27

Table 2: EICs extraction from SA and SB. The threshold on the m/z values between selected EICs and reference features was 0.0030.

203 Note that the EICs extraction did not provide information on the reference
204 features that could be identified, 0, 1, 2 or more by EIC. To allow a comparison
205 with the results of Li et al, features were extracted from the selected EICs of
206 \mathbf{X}_{sa} and \mathbf{X}_{sb} , yielding 3757 and 3531 peaks/features respectively, an average of
207 4–5 by EIC. Some integration problems were due to the different EIC shapes, as
208 observed in Figure 3. Automatic integration was easy with well-defined peaks,
209 as in Figure 4(a) and (b). On the other hand, as in Figure 4(d), automatic
210 integration failed because of the complexity of the signal -here a long RT-. Thus,
211 the visualization of an EIC can be helpful to assess the quality of integration of
212 its features. Manual integration would have recovered as accurately quantified
213 11 features which failed the automatic integration. However this result was not
214 considered any more, Li et al based their benchmark on automatic integration

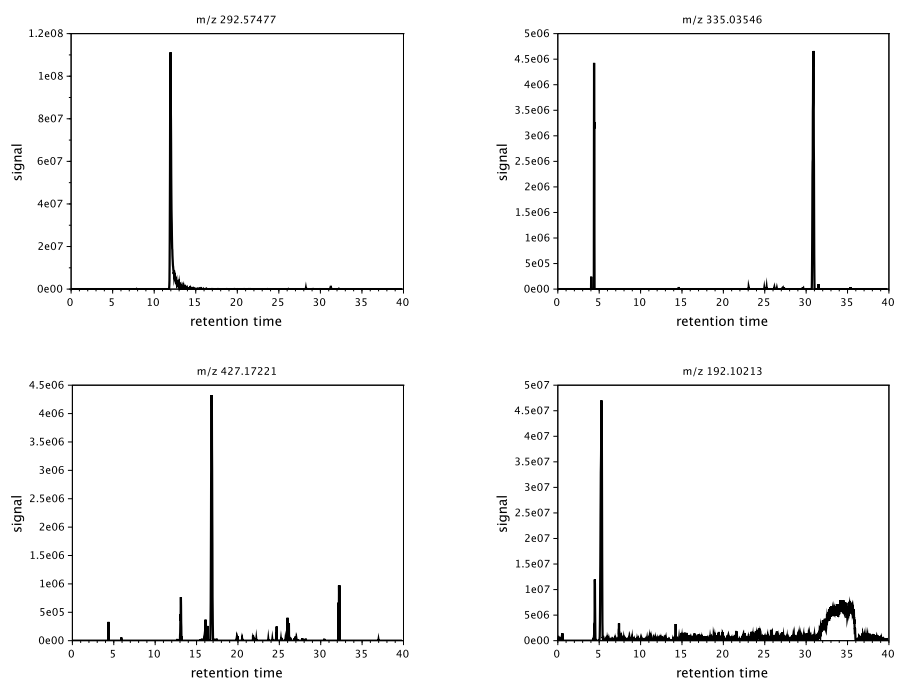
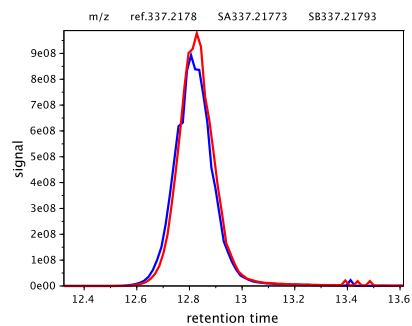
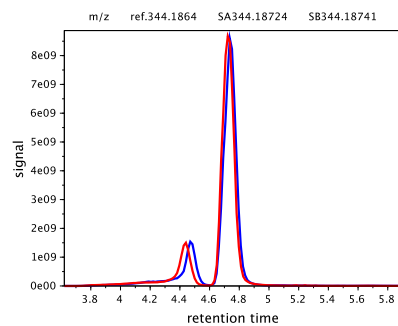


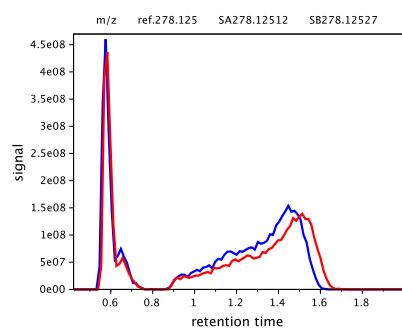
Figure 3: Dataset 2, the diversity of EICs illustrated with four examples from SA



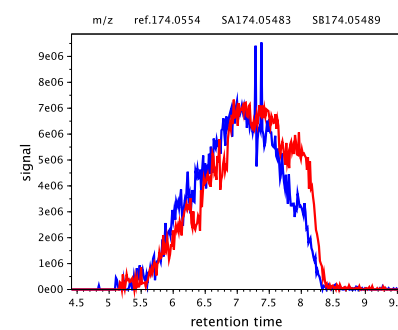
(a)



(b)



(c)



(d)

Figure 4: Dataset 2, diversity of features shapes for SA and SB in blue and red, respectively. Features (a), (b) and (c) were correctly integrated, but not for feature (d) whose RTs did not match between SA and SB.

215 and so did we. All the results concerning the features were made available as a
 216 spreadsheet file in the supplementary material. A summary is presented in table
 217 3. The numbers of true features and accurately quantified true features were
 218 820 and 787 respectively. These scores (820 – 787) were good compared to the
 219 results obtained by Li et al: 748 – 482 for Compound Discoverer, 799 – 654 for
 220 MS-Dial, 820 – 731 for XCMS and 769 – 761 for MZMine2. Then it is important
 221 to point out that Li et al tuned their algorithms with the same datasets analyzed
 222 in their paper, while we used another dataset. Their approach led to the best
 223 performance of each software, relevant for their benchmark but not in most non-
 224 targeted analysis, the reference compounds being unknown. Its simplicity of use
 225 constitutes a real added-value for the *EIC+* algorithm, even if the calculation
 226 takes time.

number of reference features	836
number of true features	820
number of accurately quantified true features	787
RMSEP of m/z values from SA ($N = 820$)	0.00042 u
RMSEP of m/z values from SB ($N = 820$)	0.00045 u
shift in RT	0.3 ± 0.1 mn

Table 3: Summary of the features extraction issued from datasets 2. Inspired from Li et al [2], the true features verify: $\Delta m/z < 0.00386$ and the reference RT fall within the experimental RT range, for both SA and SB. True features become accurately quantified when their experimental SB/SA signal ratio does not vary from more than 20 p.cent from the reference ratio. RMSEP is the root mean square error of prediction.

227 Some attention was also paid to the errors of prediction for the RTs and for
 228 the m/z values. RTs showed a shift of 0.30 minutes between our estimations
 229 and the reference RTs, see Figure 5(a), certainly due to a different calculation;
 230 our estimations were based on the median RTs. The RMSEP on m/z values
 231 were 0.00056 and 0.00052 for SA and SB respectively, but errors of prediction
 232 were lower for a majority of samples. From figure 5(b) corresponding to SA,
 233 more than 650 m/z values present differences under or equal to 0.0002. With
 234 such accuracy, the determination of raw formulae from experimental m/z values
 235 becomes possible.

236 4. Conclusion

237 Our *EIC+* algorithm presented a good recovery of true features and a good
 238 accuracy of the calculated m/z values, standing the comparison with XCMS,
 239 MZMine2 or Xcalibur. But its most interesting characteristic relies on a few
 240 (3) and self-explanatory tuning parameters, a threshold on the m/z values, a
 241 threshold on the signal intensities and a threshold on the noise estimated by
 242 the Durbin-Watson value. Less parameters means easier and more reproducible
 243 tunings. To give access to Galaxy users, the algorithm was deposited in the
 244 Galaxy Test Toolshed (<https://testtoolshed.g2.bx.psu.edu/>) where it forms a

245 suite of 9 tools. The Galaxy Test Toolshed eases the installation in a Galaxy
246 web application. The code of the 9 tools can also be downloaded via a link to
247 a Mercurial git managed by Galaxy.

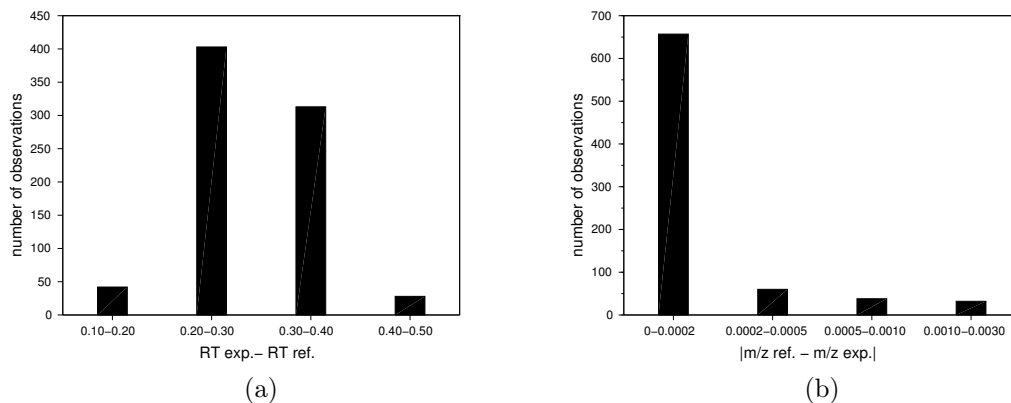


Figure 5: Number of observations in groups defined by the differences between experimental and reference values for retention times (a) and for m/z values (b)

248 5. Acknowledgement

249 This work was part of the Phenoval PRRI program funded by the Region Oc-
250 citanie, France. Thanks to Emmanuelle Meudec, Pierre-Marie Allard, Arnaud
251 Garcia, Yann Guitton and David Ropartz for useful discussions and/or pro-
252 viding datasets during the preliminary tests of this algorithm, and to Virginie
253 Rossard for support about Galaxy.

254 6.

267 7. Bibliography

- 268 [1] Jean-Claude Boulet, Emmanuelle Meudec, Anna Vallverdu-Queralt, and
269 Veronique Cheynier. Hrms: focus on the m/z values estimated by the
270 savitzky-golay first derivative. *Rapid Communications in Mass Spectrom-*
271 *etry*, doi:10.1002/rcm.9036, 2021.
- 272 [2] Zhucui Li, Yan Lu, Yufen Guo, Haijie Cao, and Qinhong Wang. Compre-
273 hensive evaluation of untargeted metabolomics data processing software in
274 feature detection, quantification and discriminating marker selection. *Ana-*
275 *lytica Chimica Acta*, 1029:50–57, 2018.
- 276 [3] Kermit K. Murray, Robert K. Boyd, Marcos N. Eberlin, G. John Langley,
277 Liang Li, and Yasuhide Naito. Definitions of terms related to mass spec-
278 trometry. *Pure and Applied Chemistry*, doi:10.1351/pac-rec-06-04-06, 2013.
- 279 [4] Owen D. Myers, Susan J. Sumner, Shuzhao Li, Stephen Barnes, and Xiuxia
280 Du. Detailed investigation and comparison of the xcms and mzmine2 chro-
281 matogram construction and chromatographic peak detection methods for
282 preprocessing mass spectrometry metabolomics data. *Analytical Chemistry*,
283 85:8689–8695, 2017.
- 284 [5] Owen D. Myers, Susan J. Sumner, Shuzhao Li, Stephen Barnes, and Xi-
285 uxia Du. One step forward for reducing false positive and false negative
286 compound identifications from mass spectrometry metabolomics data: new
287 algorithms for constructing extracted ion chromatograms and detecting chro-
288 matographic peaks. *Analytical Chemistry*, 89:8696–8703, 2017.
- 289 [6] Tomas Pluskal, Sandra Castillo, Alejandro Villar-Briones, and Matej Oresic.
290 Mzmine2: modular framework for processing, visualizing and analyzing mass
291 spectrometry-based molecular profile data. *BMC Bioinformatics*, 11(395):1–
292 11, 2010.
- 293 [7] Colin A. Smith, Elisabeth J. Want, Grace O’Maille, Ruben Abagyan, and
294 Gary Siuzdak. Xcms: processing mass spectrometry data for metabolite
295 profiling using non-linear peak alignment, matching, and identification. *An-*
296 *alytical Chemistry*, 78:779–787, 2006.
- 297 [8] Ralf Tautenhahn, Christoph Bottcher, and Steffen Newman. Highly sensitive
298 feature detection for high resolution lc/ms. *BMC Bioinformatics*, 9:504,
299 2008.
- 300 [9] Anna Vallverdù-Queralt, Emmanuelle Meudec, Matthias Eder, Rosa M.
301 Lamuela-Raventos, Nicolas Sommerer, and Véronique Cheynier. Targeted
302 filtering reduces the complexity of uhplc-orbitrap-hrms data to decipher
303 polyphenol polymerization. *Food Chemistry*, 227:255–263, 2017.

